

Current Generation in Double-Matrix Structure: A Theoretical Simulation

Regular Paper

Bogdan Lukiyaneets¹, Dariya Matulka^{1,*} and Ivan Grygorchak¹

¹ Lviv Polytechnic National University, Ukraine

* Corresponding author E-mail: dariya2009@gmail.com

Received 28 March 2013; Accepted 2 May 2013

© 2013 Lukiyaneets et al.; licensee InTech. This is an open access article distributed under the terms of the Creative Commons Attribution License (<http://creativecommons.org/licenses/by/3.0>), which permits unrestricted use, distribution, and reproduction in any medium, provided the original work is properly cited.

Abstract Peculiarities of kinetic characteristics in a supramolecular system, in particular, in a double-matrix structure observed at change of the guest content in a matrix-host are investigated. Results obtained within the framework of a time-independent one-dimensional Schrödinger equation with three barrier potential qualitatively explain experimental data. They indicate the importance of size quantization of a system, correlation between energy and geometric characteristics of both guest and host in this case.

Keywords Molecular-Lattice Structure; Intercalation, Kinetic Characteristics, Quantum Size Effect

1. Introduction

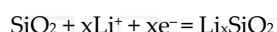
Recently, there are intensive both theoretical and experimental research in the field of new technology – nanotechnology. In contrast to traditional technologies the nanotechnology operates with materials and systems whose size at least in one crystallographic direction is from one to a hundred nanometers. These materials possess a number of unique physical properties, which are quite perspective from the viewpoint of their practical applications in electronics.

One up-to-date technical problems is the creation of new efficient autonomous generate/conversion devices and energy storage. Today transition to nanoscale objects as energy or charge storages allows to solve this problem. Really, application of the nanodispersed FeS₂ in an energy storage device with a lithium anode increases the specific capacity almost by 20% in comparison with a coarse-grained homologue [1], and the nanosized γ -Fe₂O₃ possesses the high recirculated capacity 200 mA hour/g and good cycling in a range 1.5-4.0 V regarding Li⁺/Li in comparison with the macrostructured α -Fe₂O₃, γ -Fe₂O₃ and α -Fe₃O₄ [2]. The concept of "electrochemical grafting" [3, 4] explains the effect by the features density of nanoobjects. From our point of view the nanostructural cathode material with a hierarchical architecture may be an efficient energy storage. The supramolecular and double-matrix structures belong to a broad class of nanoobjects. The supramolecular structure is structure in which two or more smaller components (guests) are introduced into larger one (host) without the formation of ordinary chemical compounds. It is possible in the case of a weak host - guest interaction. Clathrates [5], in particular relate to such structures, namely their "host-guest" interaction is based on the principle of a molecular recognition "lock - key" [6-7]. The nanostructural organization - the clathrate (or supramolecular) ensures

not only vital new interfacial charge transfer, but also the efficient Faraday storage of energy.

The current-forming phenomenon there was investigated in the molecular lattice mesoporous regular structure on the SiO_2 - MCM-41-basis [8] in the hierarchical double-matrix structure MCM-41<TiO₂> and in the supramolecular assembly of hierarchical architecture MCM-41<hydroquinone>.

The essence of a current-generation reaction in the nanoscale silica (similar in the structure TiO₂) is the reaction



The kinetics of an intercalation current generation was investigated by the impedance spectroscopy in the frequency range of 10^{-3} – 10^6 Hz. To establish the behavior of kinetic parameters in the current generation of synthesized double-matrix structures the Nyquist diagrams were applied, i.e., dependence of the imaginary part of total impedance on its real part was analyzed.

Obtained results are well simulated by the equivalent electrical circuit shown in Figure 1.

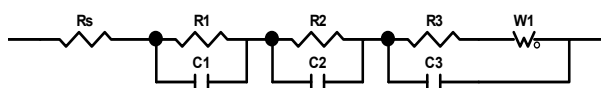


Figure 1. The generalized equivalent electrical circuit on the impedance spectroscopy basis

Here R_s is the series equivalent resistance, which contains a resistance of electrolyte; the series electric circuits $R_1||C_1$, $R_2||C_2$ and the Randles - Ershler circuit $C_3|| (R_3-W_1)$ are connected with the charge transfer through the matrix material, nematic liquid crystal, and matrix/nematic interface (molecular interlayer), respectively. Checking the adequacy of the model package of experimental data showed good results: the Kramers-Kronig coefficient did not exceed $3 \cdot 10^{-5}$.

The computer-parametric identification of the diagram is shown in Figure 2. As can be seen, the parameters R_2 , R_3 , C_2 , C_3 clearly show the unusual, oscillatory character which explicitly or implicitly (via the thermodynamic Wagner factor [9]) depend on the electron transport. There is reason to believe that such nonmonotonic dependence is caused, in particular, by the rearrangement of electronic states in the supramolecular assemblies due to the intercalant introduction. R_3 , which is connected with an ion transfer from the electrolyte to the guest's positions of cathode material, does not oscillate since it is less sensitive to the peculiarities of electron structure.

It was obtained that dependence of the lithium dissolution entropy on the guest content x in the MCM-41<hydroquinone <Li_x>> is nonmonotonic also.

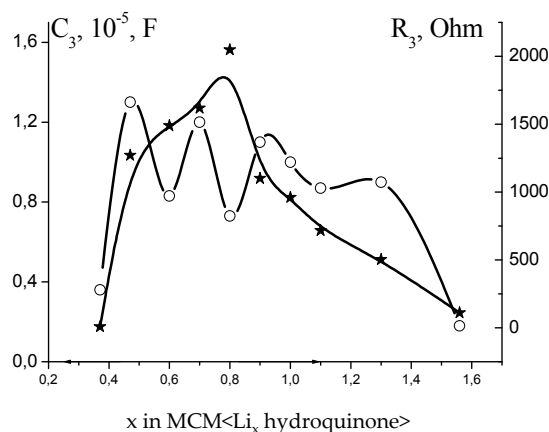
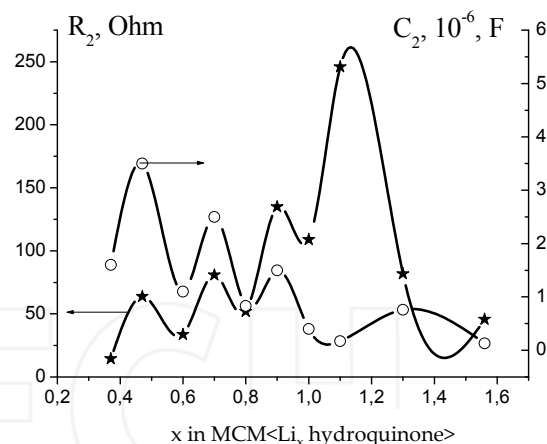


Figure 2. Change of the electric circuit parameters (R_2 , R_3 , C_2 , C_3) in the MCM-41<hydroquinone <Li_x>> depend on the guest content x

The purpose of this paper is to show the quantum mechanical nature of the nonmonotonic character of current generation in the studied objects.

2. Theoretical model

Any solid body is a potential well or a system of potential wells for an electron. Therefore, its spectrum has a discrete character. In the wide potential well these discrete energy levels are so densely arranged that the spectrum can be regarded as continuous. As soon as a body size reduces the distance between the discrete energy levels so increases that the discreteness clearly manifests itself in different physical phenomena (e.g., in an optical spectra). This phenomenon of size quantization is especially important in the low-sized bodies, in particularly, in the nanoparticles or supramolecular systems.

Information about the behavior of an electron in nanoobjects gives solution of the time-independent Schrödinger equation, namely:

$$H\psi(x) = E\psi(x) \quad (1)$$

Here $H = -\frac{\hbar^2}{2m}\nabla^2 + U(x)$ is a Hamilton operator, $U(x)$ is a potential energy of a particle with mass m (E is its total energy; \hbar is the Planck constant).

The well-known quantum-mechanical problem "a particle in infinite well"

$$U(x) = \begin{cases} \infty & x \in (-\infty; 0], [d, \infty) \\ 0 & x \in [0, d] \end{cases} \quad (2)$$

may serve as an illustration of nanoobject (d is width of the well). In this case the quantized levels of a particle are [10, 12]:

$$E_n = \frac{\hbar^2 \pi^2}{2md^2} n^2, \quad (3)$$

and the corresponding wave functions are:

$$\psi_n(x) = \sqrt{\frac{2}{d}} \sin\left(\frac{\pi n}{d} x\right), \quad (4)$$

where $n = 1, 2, 3, \dots$

From (3) it follows that the discreteness is greater for narrower wells.

Consider the electron tunneling in double-matrix or supramolecular structures. We use an one-dimensional time-independent Schrödinger equation (1) with the potential simulating such structures, namely:

$$U(x) = \begin{cases} 0, & x \in (-\infty; x_1] & \text{range 1} \\ U_b, & x \in [x_1; x_2] & \text{range 2} \\ U_a, & x \in [x_2; x_3] & \text{range 3} \\ U_c, & x \in [x_3; x_4] & \text{range 4} \\ U_a, & x \in [x_4; x_5] & \text{range 5} \\ U_b, & x \in [x_5; x_6] & \text{range 6} \\ 0, & x \in [x_6; \infty) & \text{range 7} \end{cases} \quad (5)$$

This potential is represented in Figure 3.

Here, the ranges 1-2, 5-6 describe the barrier created by the host shell and the range 3-4 with the size d_2 is a guest introduced into the host ($x_2 - x_1 = c$; $x_3 - x_2 = d_1$; $x_4 - x_3 = d_2$; $x_5 - x_4 = d_1$; $x_6 - x_5 = c$). Changing the dimensions d_2 and values of the potential U_c it is possible to simulate the amount x of introduced guest.

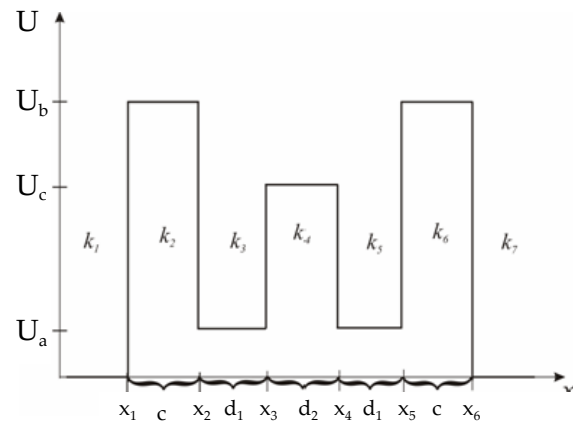


Figure 3. Potential of double-matrix structure (here x is a geometrical characteristic)

In the wells with finite thickness and height of barriers an electron is not fully localized in the wells, and there is a finite probability of its penetration outside of the wells. As a result, the energy levels have a finite width, and corresponding state is not purely stationary but quasistationary, $E_n = \text{Re } E_n + i \text{Im } E_n = E_{n1} + i E_{n2}$, with the lifetime at the level E_n $\tau_n = \frac{\hbar}{2E_{n2}}$ (E_{n1}, E_{n2} are the real and imaginary parts of E_n , respectively).

Consider two problems:

- Electron energy states within the double-matrix structure - so-called virtual state. (By analogy with the problem of "a particle in infinite well" one can predict the electron energy states as a set of levels), and
- an electron tunneling into the structure.

The solution of the 1-st problem is especially important for understanding of the 2-nd problem solution. We would remind you [12] that in the case of two-barrier structure it is probable so-called resonant tunneling. Its essence is increasing (up to 1) of the tunneling probability of an electron through both barriers if its energy coincides with any virtual levels. This situation is a result of the interference of incident and reflected waves in the interbarrier area. The phenomenon of interference should be expected in the double-matrix system. On its basis we can predict the effects of tunneling into the double-matrix structure, which is dominant in the current generation in the nanostructural electric power storages.

Let us analyze the consequences of difference between the potential (4) and the two-barrier potential for tunneling in case of the double-matrix structure.

2.1 Virtual states

The solutions of time-independent Schrödinger equation in any range of the rectangular potential are of the form:

$$\psi_l(x) = A_l \exp(k_l x) + B_l \exp(-k_l x), \quad (l = 1, 2, \dots, 7), \quad (6)$$

where the 1-st term describes an incident wave, and the 2-nd - a reflected one and A_l, B_l are their amplitudes;

$k_l = i \frac{\sqrt{2m_l^*(\epsilon_n - U(x_l))}}{\hbar}$, m_l^* is an electron effective mass in the l -th range.

For the electron placed into the double-matrix structure A_1 and B_7 are equal to zero. It means the absence of the incident wave in the 1-st range, and reflected in the 7-th range.

Let us consider the wave function (6) and its derivative

$$\Psi'_l(x) = k_l A_l \exp(k_l x) - k_l B_l \exp(-k_l x) \quad (7)$$

Taking into account the continuity condition of wave functions in any point, matching such functions in the point x_l ($l = 1, 2, 3, \dots, 6$) we obtain:

$$\begin{aligned} A_l \exp(k_l x_l) + B_l \exp(-k_l x_l) = \\ A_{l+1} \exp(k_{l+1} x_l) + B_{l+1} \exp(-k_{l+1} x_l) \end{aligned} \quad (8)$$

and from the continuity condition of their derivatives in this point we obtain:

$$\begin{aligned} k_l A_l \exp(k_l x_l) - k_l B_l \exp(-k_l x_l) = \\ k_{l+1} A_{l+1} \exp(k_{l+1} x_l) - k_{l+1} B_{l+1} \exp(-k_{l+1} x_l) \end{aligned} \quad (9)$$

Equations (8), (9) are a set of twelve homogeneous linear equations in respect to thirteen unknowns A_1, B_1, A_7, B_7 (here $l = 1, 2, 3, \dots, 6$).

According to the theory of a system of homogeneous linear equations its nontrivial solutions are realized at the equality to zero of the determinant formed from the coefficients at the unknown quantities. The obtained eigenvalues yield eigenvectors B_1, A_1, B_7, A_7 , and, consequently, the wave functions.

Recently, the alternative method for finding the energies and wave functions were widely used [13-14]. In [13] it

was observed a formal coincidence of the analytical expressions of equations describing the quantum-mechanical problem with the rectangular potentials and the transmission line problem in classical electrodynamics. The equation can be represented as a recurrence relation in the matrix form:

$$\begin{pmatrix} A_{l+1} \\ B_{l+1} \end{pmatrix} = \begin{pmatrix} \frac{1+\alpha_l}{2} \exp(k_l(x_{l+1}-x_l)) & \frac{1-\alpha_l}{2} \exp(-k_l(x_{l+1}-x_l)) \\ \frac{1-\alpha_l}{2} \exp(k_l(x_{l+1}-x_l)) & \frac{1+\alpha_l}{2} \exp(-k_l(x_{l+1}-x_l)) \end{pmatrix} \begin{pmatrix} A_l \\ B_l \end{pmatrix} \quad (10)$$

$$\text{where } \alpha_l = \frac{m_l^*}{m_{l+1}^*} \frac{k_l}{k_{l+1}}.$$

To solve the time-independent Schrödinger equation we have used the computer program [15]. It contains a package of the computer algebra Maple for the problems with the rectangular potentials on the Newton's method basis of solving of the transcendental equations.

We have analyzed the solutions of time-independent Schrödinger equation:

- depending on the potential U_c at the fixed potential U_a ($U_a = 0$) and its width d_2 ;
- depend on U_a .

We confine ourselves by the ground and the first three excited electron levels in the energy range (0 - 1.0) eV.

Consider the levels of introduced particle with the widths $d_2 = 1, 8, 15$ and 22 nm and its potential $U_c = 0.1, 0.3, 0.5$ and 0.7 eV at the constant geometrical dimensions of shell (host). As an example, Table 1 shows the values of ground and first three excited states with $U_a = 0$, $U_b = 1$ for $d_2 = 1$ nm and $d_2 = 8$ nm on the guest height U_c . Figure 4a,b shows graphical dependence of such states and squares of their wave functions on the guest height U_c for the widths $d_2 = 1$ nm and $d_2 = 8$ nm. Figure 4 c, d (Figure 4 e, f) shows the squares of wave function for various d_2 and for the same potentials $U_c = 0.1$ ($U_c = 0.7$). (For visualization in Figure 4 the normalization conditions are ignored).

	$d_2 = 1$ nm				$d_2 = 8$ nm			
	$U_c = 0.1$	$U_c = 0.3$	$U_c = 0.5$	$U_c = 0.7$	$U_c = 0.1$	$U_c = 0.3$	$U_c = 0.5$	$U_c = 0.7$
E_1	0.0104	0.0154	0.0176	0.0189	0.0254	0.2629	0.4881	0.7393
E_2	0.0217	0.0218	0.0219	0.0219	0.0266	0.2694	0.4994	0.7841
E_3	0.0558	0.0655	0.0719	0.0760	0.0929	0.3644	0.5836	0.8374
E_4	0.0870	0.0872	0.0875	0.0877	0.1046	0.4458	0.7047	0.9692

Table 1. Dependence of the ground and first three excited states on the guest height U_c for the widths $d_2 = 1$ nm and $d_2 = 8$ nm

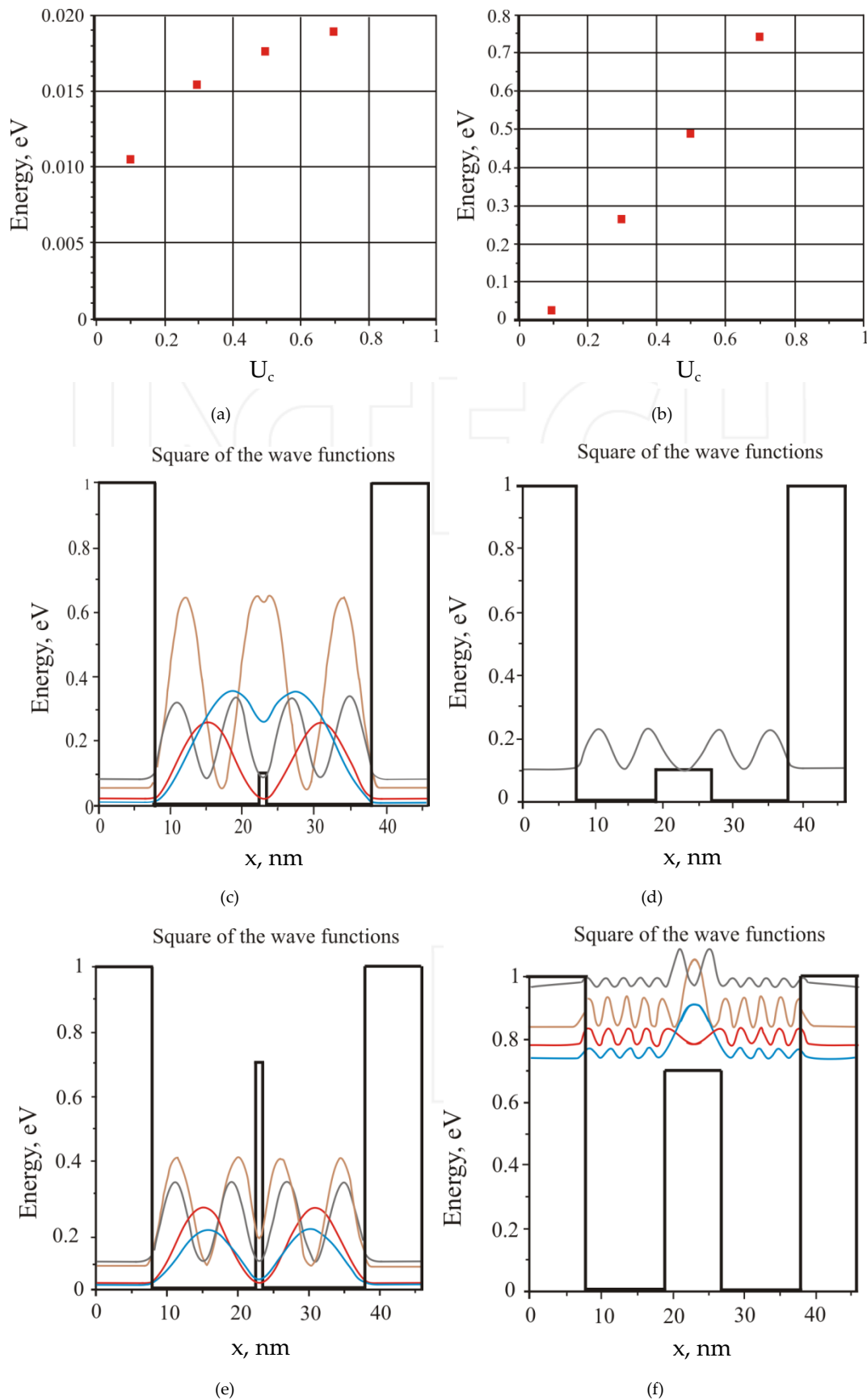


Figure 4. The ground state E_1 position depend on U_c for $d_2 = 1$ nm (a) and $d_2 = 8$ nm (b); c (d) are the squares of wave function at $d_2 = 1$ nm (for the 3-rd excited state at $d_2 = 8$ nm) and $U_c = 0.1$; e (f) are the squares of wave function for $d_2 = 1$ nm ($d_2 = 8$ nm) and $U_c = 0.7$. In all cases $U_a = 0$, $U_b = 1$. (All energy characteristic are in eV).

Let us compare effect of the guest presence in a well with the conclusions of the quantum-mechanical problem "a particle in infinite well". If in the problem "a particle in infinite well" the square of the wave function of ground state has a single maximum in the center of well, in our case this characteristic has a hollow in the same point. Thus, the square of the ground state of wave function is a curve with two symmetrical (as a result of the symmetry of chosen potentials) located maxima. The square of the wave function of first excited state qualitatively agrees with an analogous one in the problem "a particle in infinite well". The only difference is a position of maximum in the first and second cases. Particularly evident changes at the consideration of the same problem take place at the higher values of the potential U_c , namely at $U_c = 0.7$ (see Figure 4e). Specific changes occur also with the d_2 width increasing of the barrier U_c . At the same time the comparing of the results with the results of the problem "particle in an infinitely well" is less obvious (see Figure 4f).

The increasing of the barrier thickness d_2 simultaneously is accompanied by the narrowing of wells on both sides U_c , reducing overlap of the wave functions between them. Therefore, these wells can be regarded as independent. The narrowing of wells itself causes a shift of the levels to the higher values. Such conclusion is confirmed by similar calculations $E_1(U_c)$ for the cases $d_2 = 15$ and 22 nm. At constant value of the guest potential U_c ($U_c = 1$) the monotonic increase of all levels is observed with the increasing of the bottom of the potential U_c ($U_b = 1$, $d_2 = 1$ nm).

Table 2 shows the values of levels depending on the height of the well U_a at $d_2 = 8$ nm, and Figure 5 is a graphical representation of ground state level as a function of the height U_a of the well. The absence of values is the fact that some electron states are above the range of our calculations, $E \leq 1$ eV. The increasing U_a leads to the increase of tunneling probability. In extreme case, when the position U_a is minimal ($U_a = 0$) the tunneling grows. Obviously, the tunneling will be higher at lower $U_c - U_a$. In other words, a system of the wells can be regarded as the sum of the independent wells at $U_a = 0$ and single well of the host value at $U_a \approx U_c$.

Such circumstances may explain it would seem the strange change $E_1(U_a)$. As the depth of wells decreases (with the increasing U_a) the levels in these wells are shifted. At some value of depth upper levels will go beyond observed range of calculation. However, further reduction of depth is accompanied by the increase of tunneling. Thus, the reducing of the depth of wells may be considered as the effective width of guest well that equals from about $2d_1$ at $U_a = 0$ to $2d_1 + d_2$ at $U_a \geq U_c$.

Consequently, the levels (according to the $E \approx \frac{1}{d_{\text{eff}}^2}$) will drop to the bottom of host. It explains the increase of the levels with the increasing U_a .

	$U_a = 0.1$	$U_a = 0.3$	$U_a = 0.5$	$U_a = 0.7$
E_1	----	0.9300	0.8938	0.7939
E_2	----	-----	----	0.9034
E_3	----	----	----	----
E_4	----	----	----	----

Table 2. Dependence of energy levels on the potential U_a

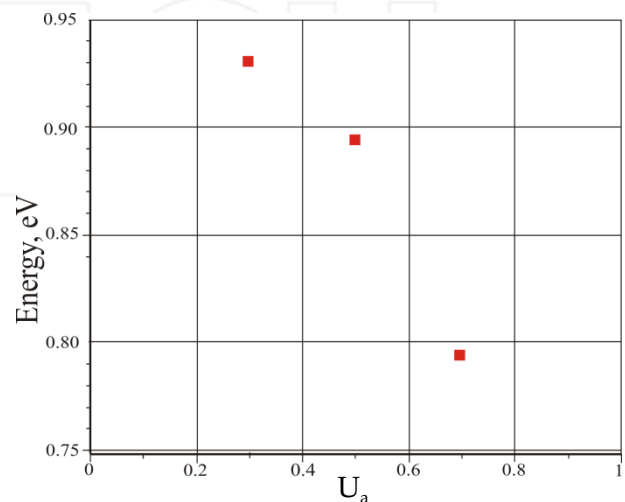


Figure 5. The ground state position as a function of the height well U_a .

Figure 6 shows the energy states and corresponding squares of the wave functions on the background of the double-matrix potential relief at $U_c = 1$, $U_a = 0.1$, $U_b = 1$, $d_2 = 1$ nm

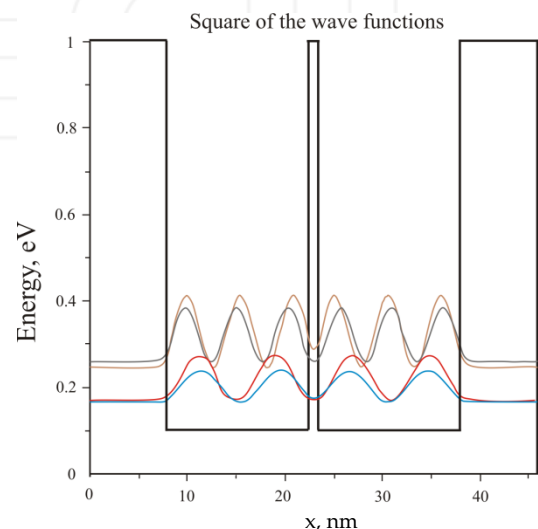


Figure 6. Square of wave function at $U_a = 0.1$ ($U_b = 1$, $U_c = 1$, $d_2 = 1$ nm).

	$U_c=0.1$	$U_c=0.3$	$U_c=0.5$	$U_c=0.7$
E_I	$9.8188 \cdot 10^{-13}$	$2.3565 \cdot 10^{-12}$	$6.1830 \cdot 10^{-9}$	$2.7544 \cdot 10^{-7}$

Table 3. The imaginary part of ground state as a function of U_c

Table 3 shows the imaginary part of ground state as a function of U_c at a thickness of $d = 1$ nm.

2.2 Tunnelling

In the problem of the left to right motion of an electron its tunneling from the range 1 to the ranges 3 and 5 are described by the relations $a_3 = \left| \frac{A_3}{A_1} \right|^2$ and $a_5 = \left| \frac{A_5}{A_1} \right|^2$, respectively.

The division of equations (8) and (9) in A_1 , transforms them into a system of the linear inhomogeneous equations relative to $a_2 = \frac{A_2}{A_1}, a_3 = \frac{A_3}{A_1}, \dots, a_7 = \frac{A_7}{A_1}, b_1 = \frac{B_1}{A_1}, \dots, b_6 = \frac{B_6}{A_1}$ with free, non-zero terms $-\exp(k_1 x_1), k_1 \exp(k_1 x_1)$ obtained at the matching of wave functions and their derivatives at the point x_1 . Then one can use the methods solving of such equations (e.g., Cramer's rule method [16]). As a result, we obtained the dependence $a_3 = \left| \frac{A_3}{A_1} \right|^2$ and $a_5 = \left| \frac{A_5}{A_1} \right|^2$ on the energy of incident electron. This

dependence is nonmonotonic. Its minima are reached at the coincidence of electron energy levels with the virtual ones, i.e. when the interference phenomena is particularly evident. Non-triviality of the manifestations of these phenomena are that for some values of the electron energy $a_5 = \left| \frac{A_5}{A_1} \right|^2$ is greater than $a_3 = \left| \frac{A_3}{A_1} \right|^2$.

The tendency of the dependences shown in Figure 7 is obvious: the tunneling increases when the electron energy tends to the value of barrier heights.

The nonmonotonic dependence of tunneling probability is obtained by the varying of incident electron energy relative to the fixed virtual states. A similar behavior of tunneling is possible with the shift of the virtual states relative the fixed incident electron energy. Such a shift is possible because the changes geometric and/or energy parameters of double-matrix structure. But such shift can be achieved, in particular, by change of the guest content in the structure.

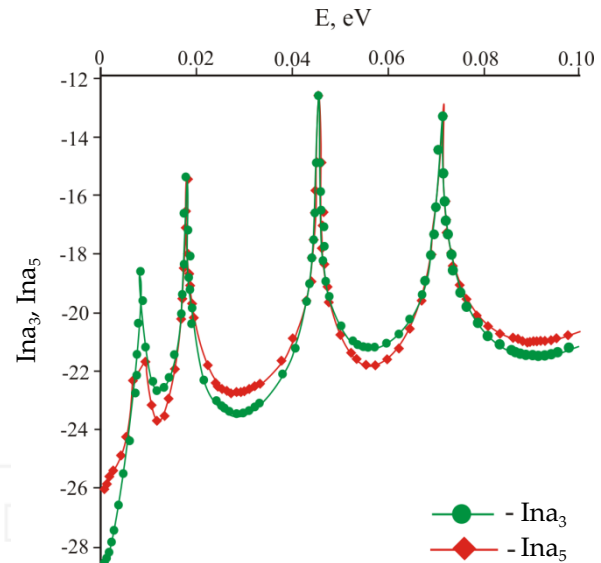


Figure 7. Dependence of tunneling probability on energy

3. Conclusions

The main result of the paper is the non-monotonic variation of electron tunneling into the host. Since the tunneling determines the current generation phenomenon of double-matrix structure, the result can be regarded as an explanation for the experimentally observed nonmonotonic behavior of current generation characteristics (see Figure 2).

We especially note:

- the importance of the size quantization in this effect;
- the effect to a greater extent is determined by the ratio between the electron virtual states and the bombarding electrons energy than by only their individual parameters.

4. References

- [1] A. Skundin, O. Efimov, O. Yarmolenko, *The state-of-the-art and prospects for the development of rechargeable lithium batteries*, vol. 71. Russ. Chem. Rev., 2002, pp. 329–346.
- [2] L. Kanevskii, V. Dubasova, *Degradation of Lithium-ion batteries and how to fight it*, vol.41. A Review Russ. J. Electrochem., 2005, pp. 1-16.
- [3] Y. Shao-Horn, S. Osmialowski, C. H. Quinn, *Nano-FeS₂ for commercial LiOFeS₂ primary batteries*, vol. 149. J. Electrochem. Soc., 2002, pp. A1499- A1502.
- [4] M. Quintin, O. Devos, M.H. Delville, G. Campet, *Study of the lithium insertion–deinsertion mechanism in nanocrystalline γ -Fe₂O₃ electrodes by means of electrochemical impedance spectroscopy*, vol. 51. Electrochim. Acta, 2006, pp. 6426-6434.
- [5] Yu. Dyadin, *Supramolecular Chemistry: clathrate compounds*, vol.2, Sorosovskii Obrazovatelnyj Zhurnal, 1998, pp. 80-88, (in Russian).

- [6] J. Lehn, *Supramolecular chemistry: concepts and perspectives*, (Wiley-VCH), 1995, p 271
- [7] J. Steed, J. Atwood, *Supramolecular chemistry*, (John Wiley & Sons, Ltd), 2000, p 970
- [8] C. Peter, *Novel Coassembly Route to Cu-SiO₂ MCM-41-like mesoporous materials*, vol. 26, Amer. Chem. Soc. 26, 2004, P. 2879-2882.
- [9] N. Korovin, *Intercalation into cathodic materials: the chemical diffusion coefficient for lithium ions*, vol. 35, Russ. J. Electrochem., 1999, pp. 661-668
- [10] A. Davydov, *Quantum mechanics*, (Pergamon) 1965
- [12] D. Bohm *Quantum theory* (N.Y.: Prentice Hall, Inc.) 1952
- [13] A. Khondker, M. Khan, A. Anwar, *Transmission line analogy of resonance tunneling phenomena: The generalized impedance concept*, vol.63, J. Appl. Phys, 1988, pp. 5191-5193.
- [14] E. Nelin, *Impedance model for quantum-mechanical barrier problems*, vol.50, Phys.-Usp. 2007, 293
- [15] A. Trofimchuk, *Simulating of electron resonance tunneling through the quantum cascade suoerlattice structures* (<http://www.exponenta.ru>), 2003
- [16] G. Korn, T. Korn, *Mathematical handbook for scientists and engineers* (McGraw-Hill Book Co, N.Y.-Toronto-London), 1961

INTECH

INTECH